Supporting Information

Pore with Gate - Enhancement of the Isosteric Heat of Adsorption of Dihydrogen *via* Post-synthetic Cation Exchange

Sihai Yang,[1] Gregory S. B. Martin,[1] Jeremy J. Titman,[1] Alexander J. Blake,[1] David R. Allan,[2] Neil R. Champness[1]* and Martin Schröder[1]*

1. School of Chemistry, University of Nottingham, University Park, Nottingham NG7 2RD (UK)
   Fax: +44 115 951 3563 E-mail: Neil.Champness@nottingham.ac.uk; m.schroder@nottingham.ac.uk

2. Diamond Light Source, Harwell Science and Innovation Campus, Didcot, Oxfordshire, OX11 0DE (UK)

1. Experimental section

1.1 Materials and Measurements.

Analyses for C, H, and N were carried out on a CE-440 elemental analyzer. Thermogravimetric analyses (TGA) were performed under a N_2 atmosphere (100 ml/min) using a TA SDT-600 thermogravimetric analyzer with a heating rate of 2 °C/min. The *in-situ* IR spectra were recorded using a Bruker TENSER 27 FT-IR spectrophotometer in KBr mode under He flow with heating rate 20 °C/min. Analyses for Li and In were carried out using an ICP-MAS analyzer. Calibration curves for ICP-MAS were prepared by dilution of commercially available standards with the sample dissolved in concentrated HNO_3, and diluted to an appropriate concentration for measurement. Powder X-ray diffraction (PXRD) data were collected over the 2θ range 4-50^o on a Bruker Advanced D8 diffractometer using Cu-Kα1 radiation (λ = 1.5406 Å, 40 kV/40mA).

1.2 ^{7}Li solid-state NMR measurements.

Table 1s. Isotropic shifts □ (in ppm) and quadrupolar coupling constants C_Q (in kHz) from solid-state ^{7}Li NMR spectroscopy.

Sample	δ(Li) / ppm	$C_q(^7Li)$ / kHz
NOTT-201-solv	-3.4(0.2)	50(2)
NOTT-201a	-2.1(0.2)	145(2)
NOTT-207-solv	-3.6(0.2)	-[a]
NOTT-207a	-2.6(0.2)	-[a]
NOTT-209-solv	-3.6(0.2)	47(2)
NOTT-209a	-2.4(0.2)	145(2)

[a] ^{7}Li satellite lines are not resolved from the central transition in this case.

2. Additional views of single crystal X-ray structures.

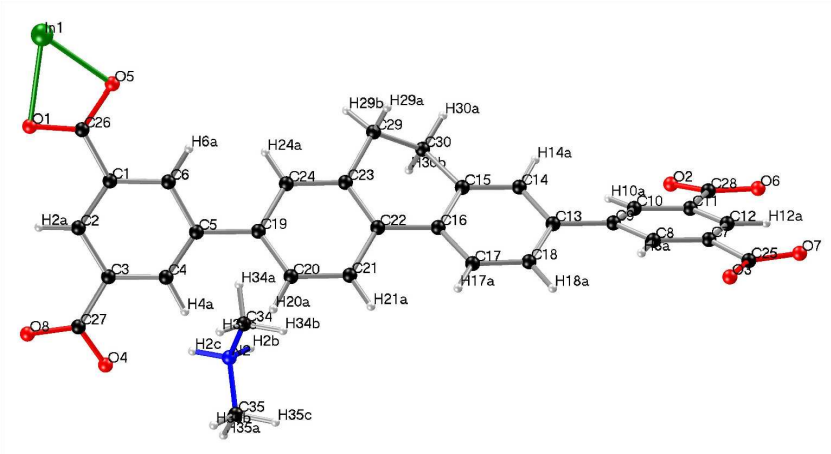

Figure 1s. View of the asymmetric units for NOTT-206-solv.

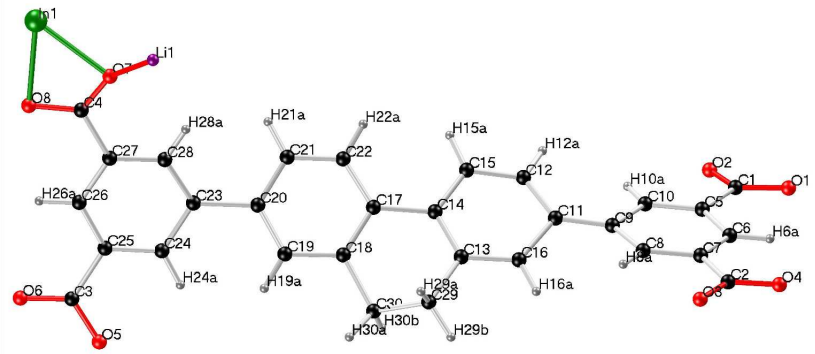

Figure 2s. View of the asymmetric units for NOTT-207-solv.

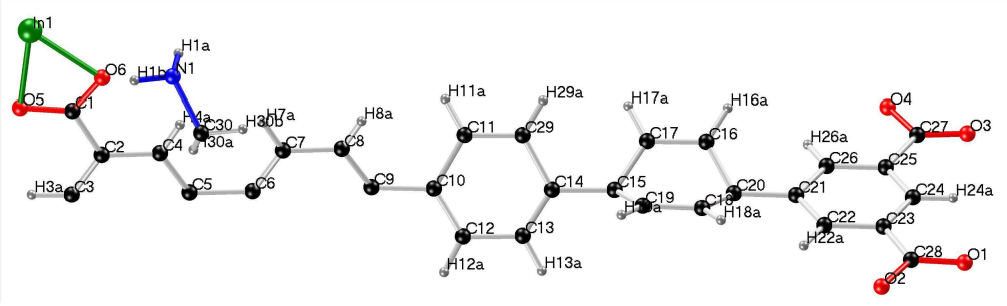

Figure 3s. View of the asymmetric units for NOTT-208-solv.

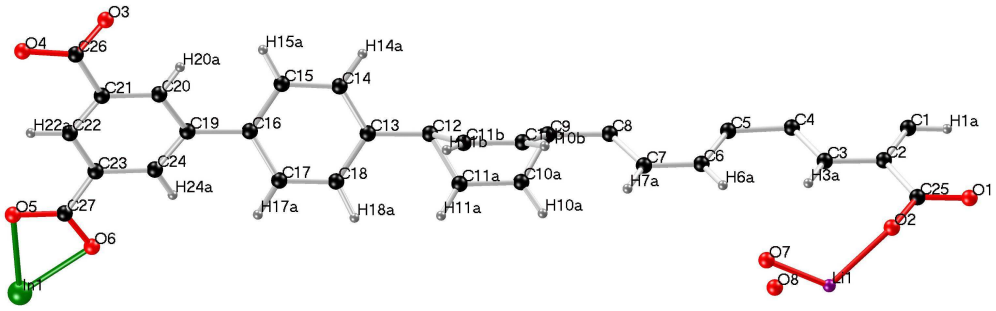

Figure 4s. View of the asymmetric units for NOTT-209-solv.

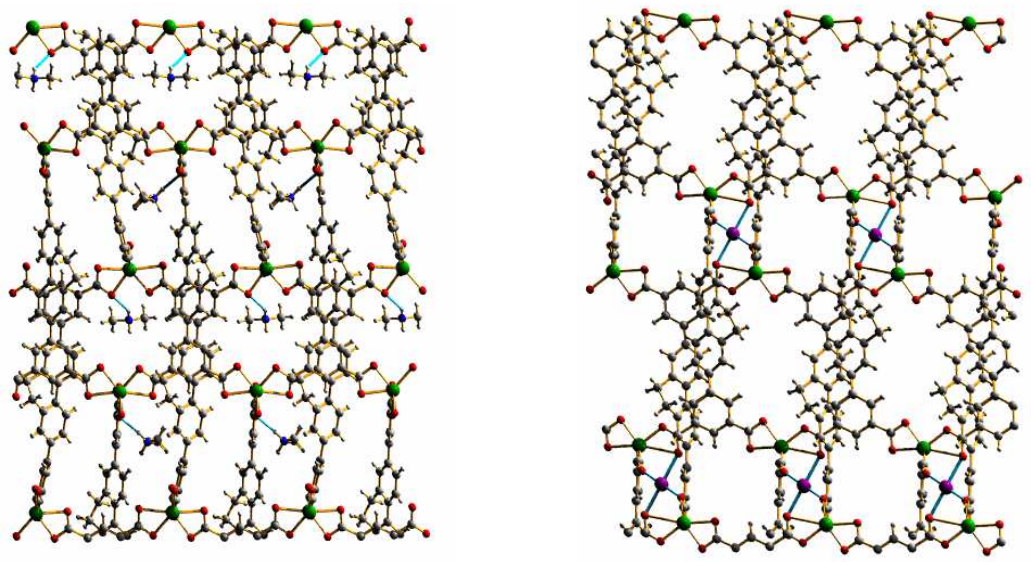

a b

Figure 5s. View of the framework structures of (a) NOTT-206 and (b) NOTT-207 along the *b*-axis.

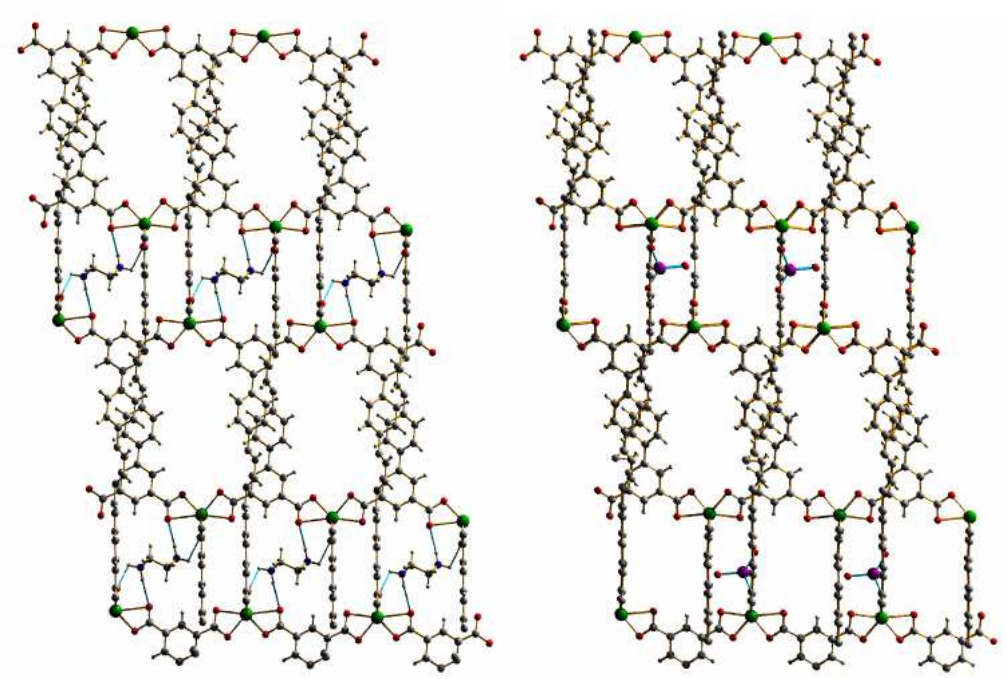

a b

Figure 6s. Views of the framework structures of (a) NOTT-208 and (b) NOTT-209 along the *b*-axis.

3. TGA plots.

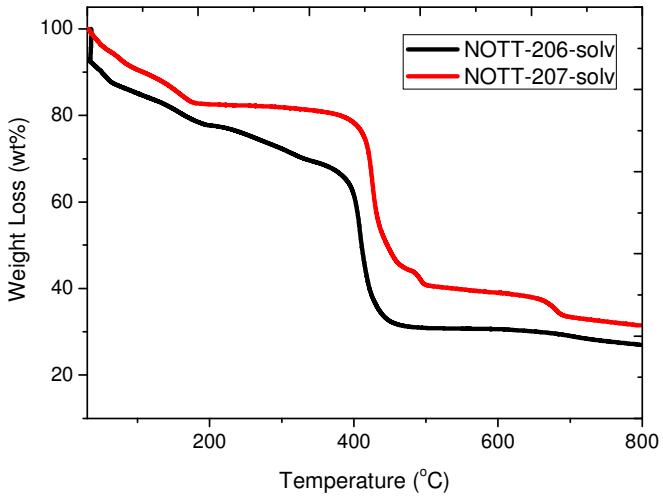

Figure 7s. TGA plots for NOTT-206-solv and NOTT-207-solv.

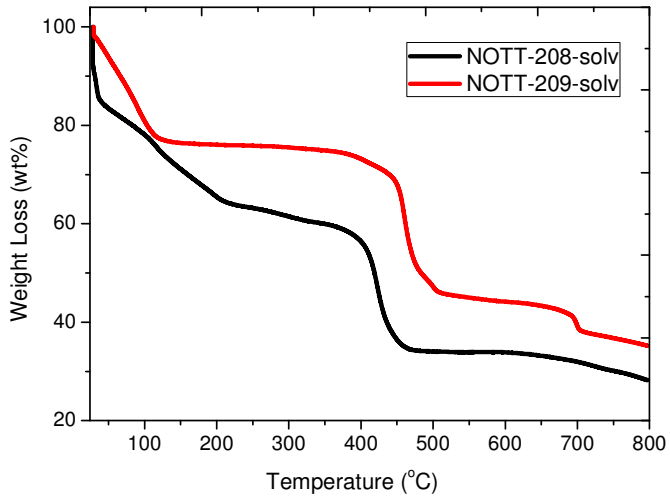

Figure 8s. TGA plots for NOTT-208-solv and NOTT-209-solv.

4. Powder X-Ray diffraction.

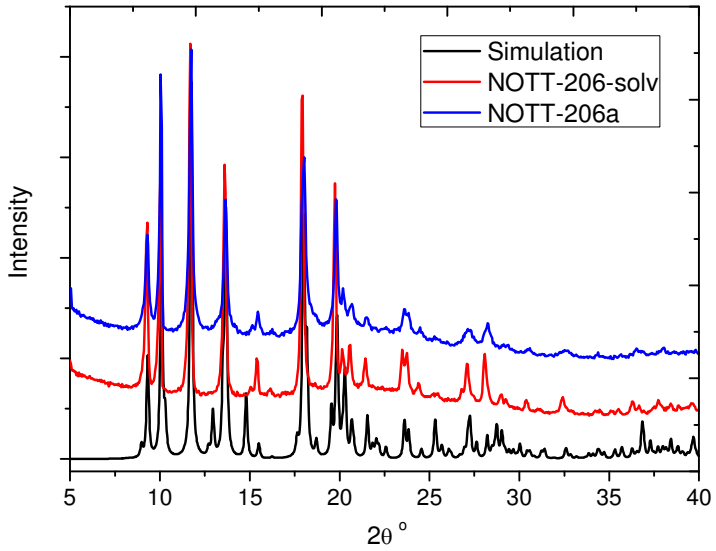

Figure 9s. Simulated and experimental PXRD patterns for NOTT-206-solv and NOTT-206a.

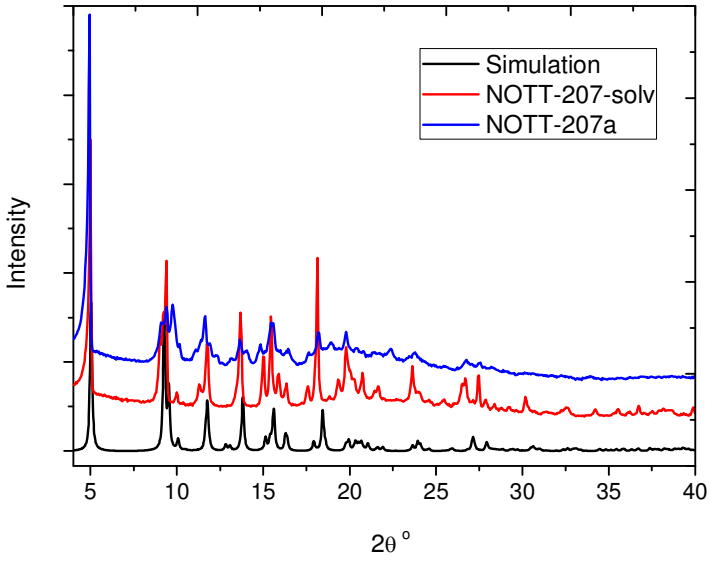

Figure 10s. Simulated and experimental PXRD patterns for NOTT-207-solv and NOTT-207a.

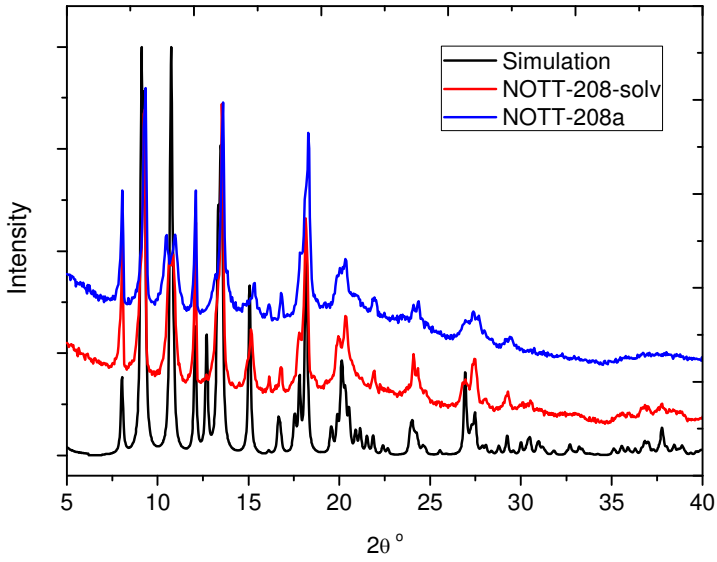

Figure 11s. Simulated and experimental PXRD patterns for NOTT-208-solv and NOTT-208a.

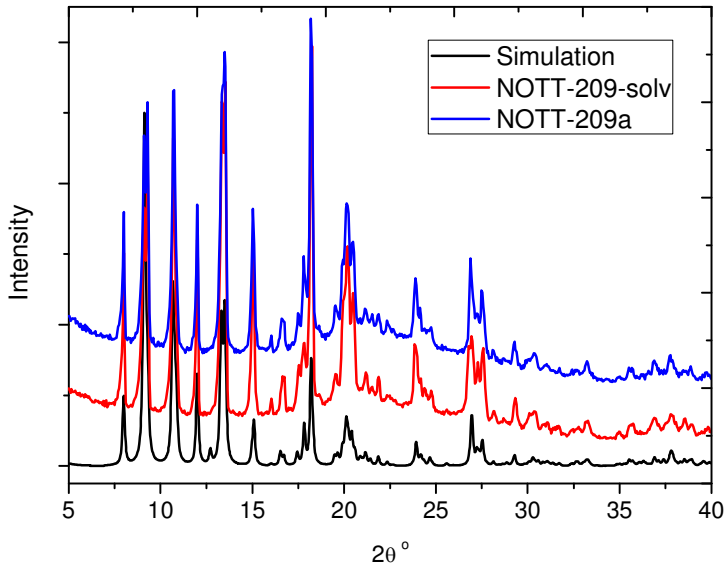

Figure 12s. Simulated and experimental PXRD patterns for NOTT-209-solv and NOTT-209a.

6. Additional gas adsorption isotherms.

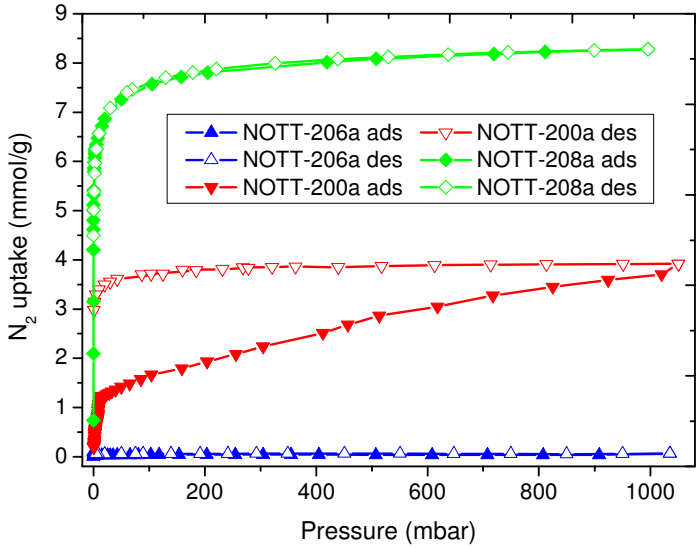

Figure 13s. N_2 sorption isotherms at 77 K for NOTT-206a, NOTT-200a and NOTT-208a.

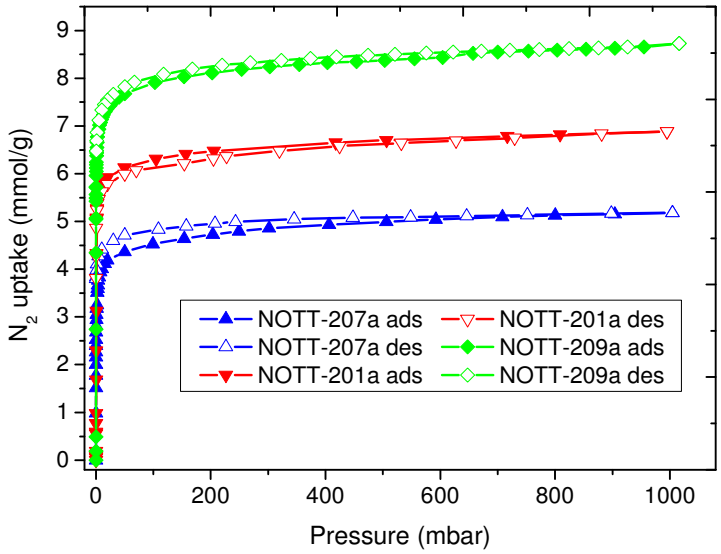

Figure 14s. N_2 sorption isotherms at 77 K for NOTT-207a, NOTT-201a and NOTT-209a.

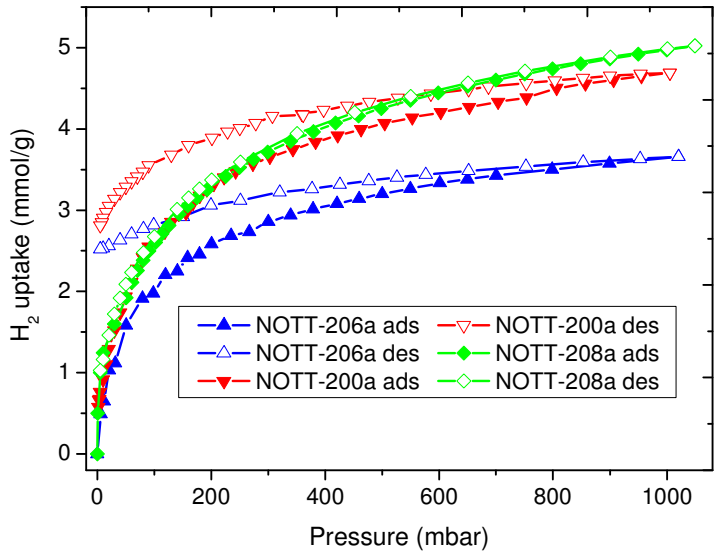

Figure 15s. H_2 sorption isotherms at 77 K for NOTT-206a, NOTT-200a and NOTT-208a.

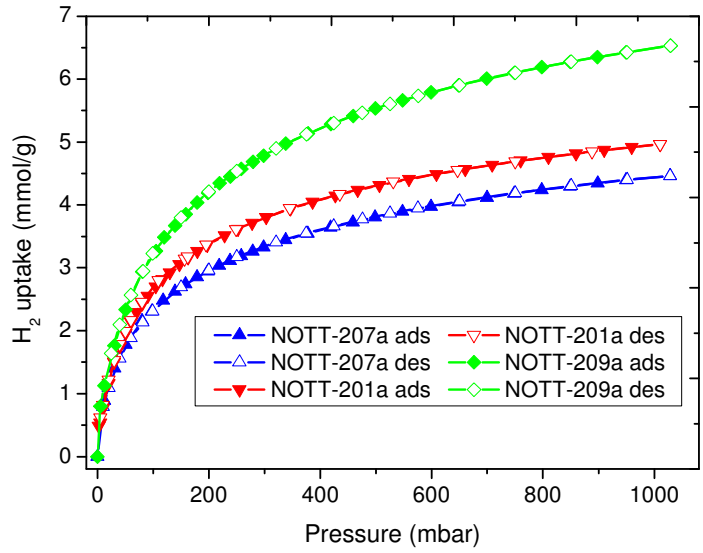

Figure 16s. H_2 sorption isotherms at 77 K for NOTT-207a, NOTT-201a and NOTT-209a.

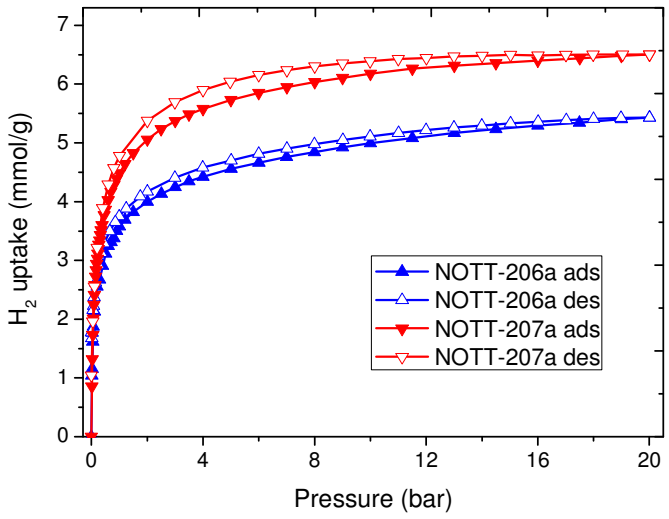

Figure 17s. High pressure (up to 20 bar) H_2 sorption isotherms at 77 K for NOTT-206a and NOTT-207a.

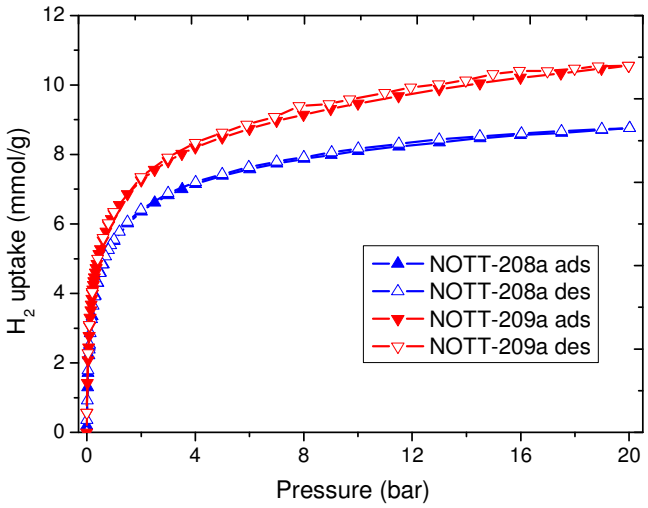

Figure 18s. High pressure (up up to 20 bar) H_2 sorption isotherms at 77 K for NOTT-208a and NOTT-209a.

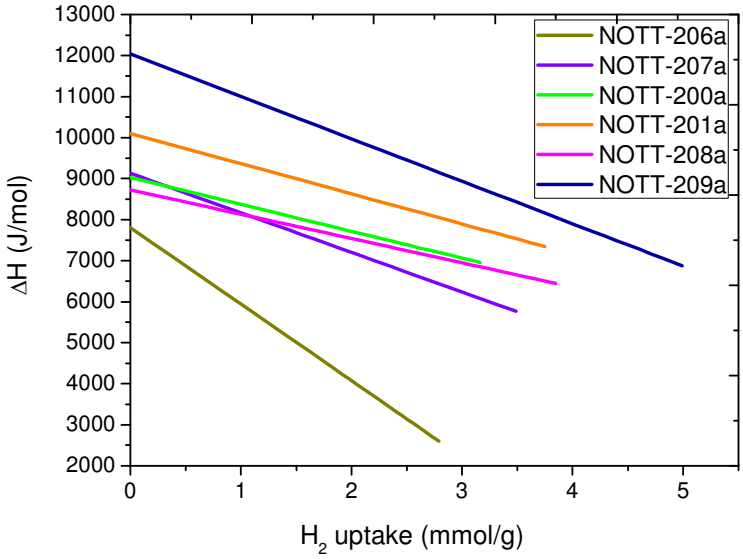

Figure 19s. Isosteric heats of adsorption of H_2 in NOTT-206a, NOTT-207a, NOTT-200a, NOTT-201a, NOTT-208a and NOTT-209a.

7. Simulation of H_2 adsorption enthalpies.

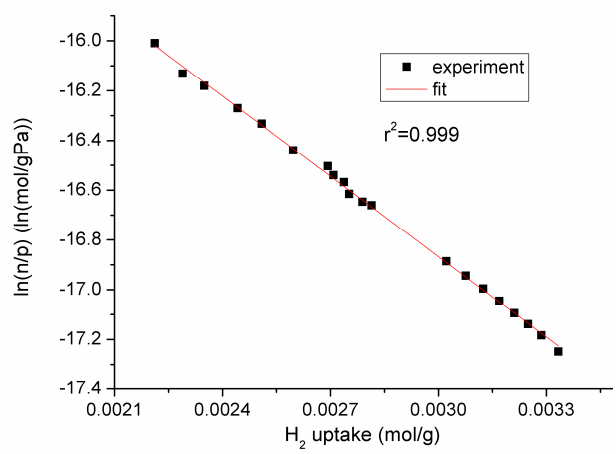

Figure 20s. Virial plot for the adsorption of H_2 on NOTT-206a at 77 K.

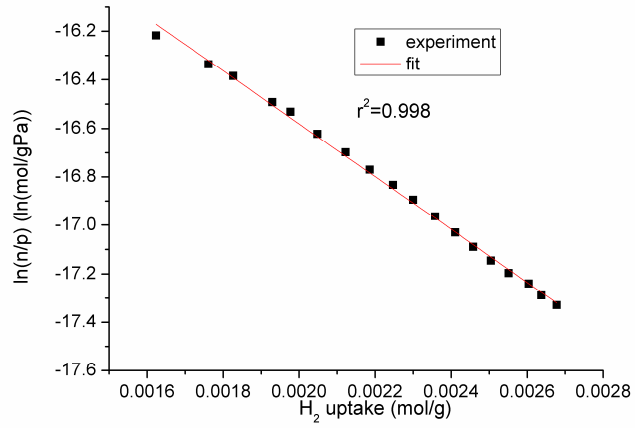

Figure 21s. Virial plot for the adsorption of H_2 on NOTT-206a at 87 K.

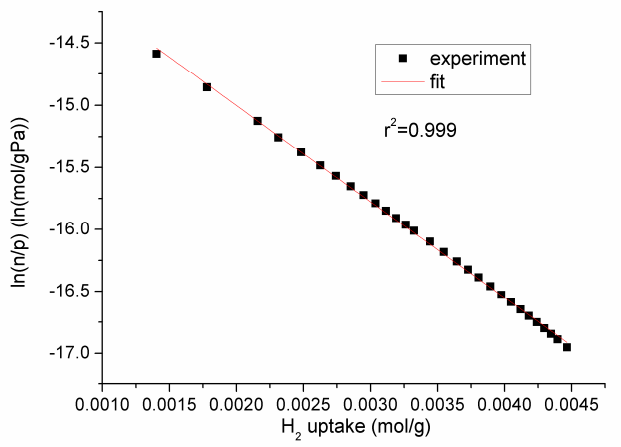

Figure 22s. Virial plot for the adsorption of H_2 on NOTT-207a at 77 K.

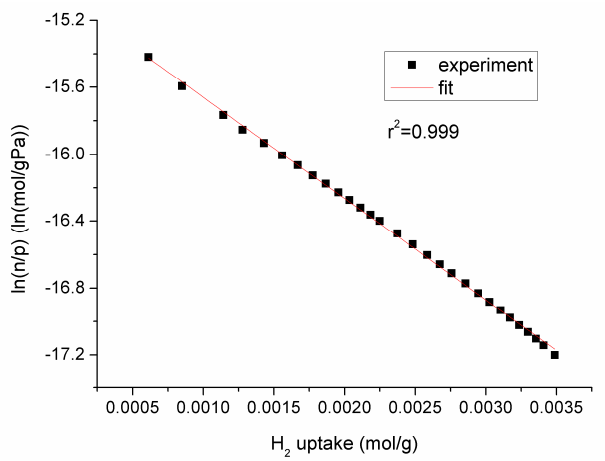

Figure 23s. Virial plot for the adsorption of H_2 on NOTT-207a at 87 K.

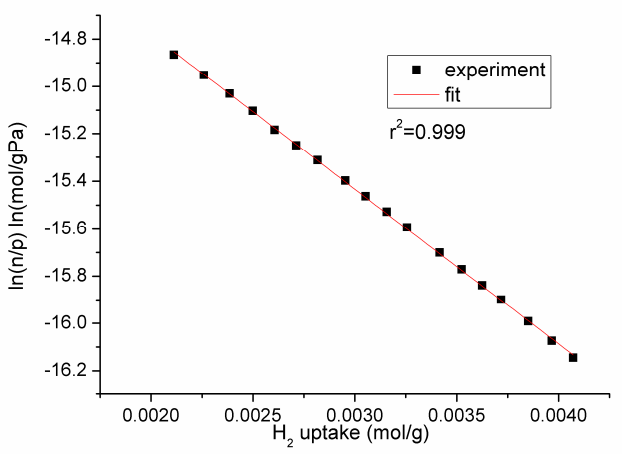

Figure 24s. Virial plot for the adsorption of H_2 on NOTT-208a at 77 K.

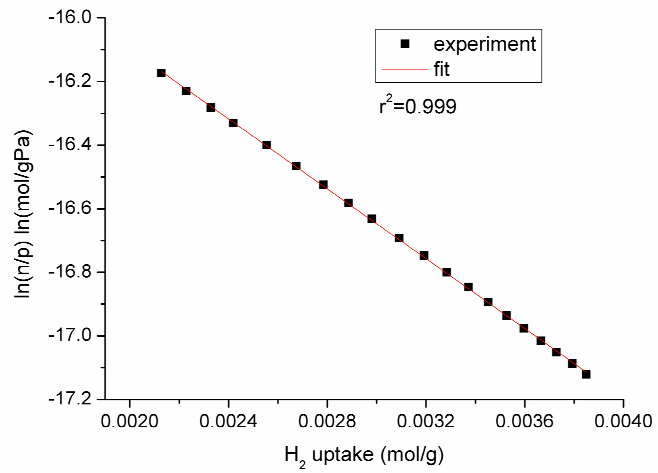

Figure 25s. Virial plot for the adsorption of H_2 on NOTT-208a at 87 K.

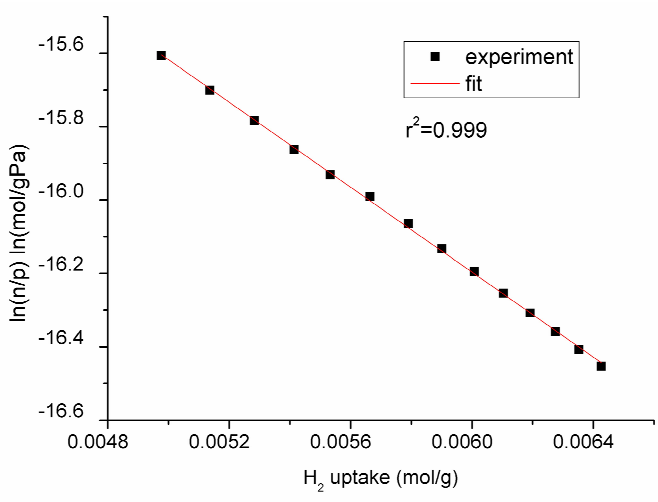

Figure 26s. Virial plot for the adsorption of H_2 on NOTT-209a at 77 K.

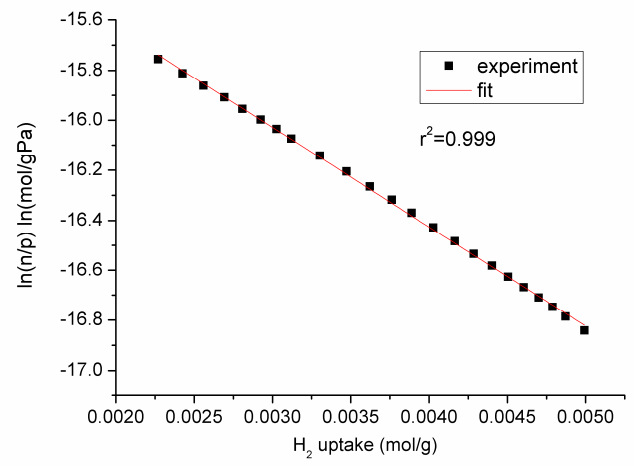

Figure 27s. Virial plot for the adsorption of H_2 on NOTT-209a at 87 K.